MOLECULAR BEAM PHOTOELECTRON SPECTROSCOPY OF $Ni(CO)_4$

J.E. REUTT, L.S. WANG, Y.T. LEE and D.A. SHIRLEY

Materials and Molecular Research Division, Lawrence Berkeley Laboratory, and Department of Chemistry, University of California, Berkeley, CA 94720, USA

Received 10 January 1986; in final form 28 February 1986

The nickel carbonyl HeI (21.2175 eV) photoelectron spectrum has been reinvestigated with improved resolution and molecular beam sampling. The $9T_2$ and 2E photoelectron bands are shown to be intrinsically diffuse, which is attributed to D_{2d} geometries. The ordering of the next seven outer valence electronic states is proposed from a linear least-squares fit of the spectrum.

1. Introduction

Transition metal carbonyls are among the most photochemically active transition metal complexes known. It is widely accepted that the bonding of these systems is described by a synergic combination of ligand-to-metal σ bonding and metal-to-ligand π backbonding [1]. The relative importance of the σ and π bonding, however, is not firmly established.

Various theoretical and experimental studies have attempted to assess the nature of the transition metal–carbonyl bond. The molecular orbital calculations have generally upheld the metal-to-ligand π-bonding contribution, but have not agreed upon its relative magnitude [2–5]. The principal experimental evidence for π backbonding has been derived from the vibrational spectroscopy [6] and bond length determinations [7] of the neutral transition metal carbonyls. Because the bonding interaction is synergic, however, a clear distinction between σ and π contributions has not been made.

Molecular photoelectron spectroscopy is a powerful method for testing bonding contributions from individual molecular orbitals. Emission of an electron from an occupied molecular orbital is accompanied by a change in geometry and force constants for the resulting ion, indicative of the bonding nature of the molecular orbital. These changes may be evaluated from the photoelectron band. Recently Hubbard and Lichtenberger have obtained high-resolution photoelectron spectra of the chromium, molybdenum, and tungsten hexacarbonyls [8]. A vibrational analysis of the T_{2g} photoelectron bands, enhanced by derivative, residual, and Fourier methods of data analysis, revealed significant π-backbonding contributions in these systems.

The transition metal carbonyls possess very soft (80–100 cm^{-1}) bending modes that will be significantly populated in room temperature samples. All photoelectron spectroscopic investigations to date have employed thermal samples and resulted in diffuse photoelectron band shapes. Although Hubbard and Lichtenberger were able to distinguish vibrational structure, their reported vibrational features were significantly broader than their reported instrumental resolution. The question remains, therefore, whether the photoelectron bands are intrinsically diffuse, or trivially broadened by hot rotational and vibrational structure, i.e. whether the broadening is homogeneous or inhomogeneous.

In this paper we report the high-resolution (12 meV) HeI (21.2175 eV) photoelectron spectrum of nickel carbonyl, which has been rotationally and vibrationally cooled in a supersonic molecular beam. Despite the improved resolution and cold sample temperature, the $9T_2$ and 2E photoelectron bands, the "nickel d bands", exhibited no vibrational fine structure. The bands appear to be intrinsically diffuse,

0 009-2614/86/$ 03.50

which may be explained by a strong distortion from the tetrahedral geometry of the neutral species. The next seven valence photoelectron bands originating from the loss of electrons from primarily ligand molecular orbitals are reported. Their ordering is proposed on the basis of relative intensity arguments.

2. Experimental

The molecular beam photoelectron spectrometer used in this experiment has been described in detail [9] and will be discussed only briefly. The electron energy analyzer consisted of a double electrostatic deflector operated at a pass energy of 1.0 eV which sampled the photoelectrons at an angle of 90° with respect to the incident photon beam. The HeI (21.2175 eV) spectrum of $Ni(CO)_4$ (Pressure Chemical Co.) was recorded with multi-channel detection at a resolution of 12 meV fwhm, as measured for $^2P_{3/2}$ lines of Ar and Xe.

Guidance for the appropriate molecular beam expansion conditions was obtained from previous molecular beam diagnostics reported in the literature. Amirav, Even and Jortner studied the internal temperatures of heavy molecules (MW = 158–398 amu) seeded in a molecular beam with laser fluorescence excitation spectroscopy [10]. They measured $T_{rot} \approx 7$ K and $T_{vib} \leqslant 50$ K of the low-frequency modes for a range of seeded beam conditions: $P_0D = 200$ Torr cm in helium, $P_0D = 25$ Tor cm in neon, $P_0D = 2.4$–3.0 Torr cm in argon, $P_0D = 2.0$ Torr cm in krypton, and $P_0D = 1.4$ Torr cm in xenon. A rare gas carrier with $M_{seed}/M_{carrier} < 50$ was shown to be necessary to produce ultra-cold samples under moderate expansion conditions. Molecular beam diagnostics of CH_4 and SF_6, two molecules that possess smaller collisional cross sections than $Ni(CO)_4$, but are also highly symmetric, and other small molecules have been reported by Luijks, Stolte and Reuss [11,12]. These Raman measurements were performed on unseeded beams at moderate expansion conditions, yet still exhibited ultracold rotational temperatures and significant vibrational cooling ($T_{vib}/T_0 \approx 0.5$) for low-frequency vibrational modes.

The present results were obtained by expanding a 10% $Ni(CO)_4$/neon mixture at 650 Torr through a 100 μm diameter nozzle at room temperature. Although no direct measurement was made of the internal temperatures of the beam, we estimate $T_{rot} \approx 20$ K and $T_{vib_i} < 75$ K for the low-frequency bending modes ($\nu_i < 350$ cm^{-1}). Spectra acquired for the $9T_2$ photoelectron band under harder beam expansion conditions (5% $Ni(CO)_4$/neon with $P_0D = 8.0$ Torr cm and 4% $Ni(CO)_4$/argon with $P_0D = 2.0, 4.0$ and 8.0 Torr cm) elucidated no additional vibrational structure.

The presence of weakly bound $[Ni(CO)_4]_x$ clusters was also tested with 584 Å photoionization and a quadrupole mass filter (Extranuclear Laboratories). Mass spectral contributions from the fragment ion Ni_2^+ were used to test the extent of clustering in the beam. For the presently reported neon-seeded beams of $Ni(CO)_4$, a cluster presence of <1% was detected. Only for the argon-seeded beams was significant (3–5%) clustering observed.

To improve statistics and allow for a frequent recalibration of the energy scale with argon and xenon, the photoelectron spectrum was obtained as a series of short 1.5 h scans, which were subsequently combined. The reported $9T_2$ and 2E photoelectron bands represent a summation of twenty-one spectra, recorded sequentially. The photoelectron bands primarily associated with the ligand orbitals were obtained by a summation of seven separate scans. These conditions permit an accuracy of ±5 meV in the measurement of absolute ionization potentials. Peak splittings reduce systematic error and may be reported with higher accuracy.

3. Results and discussion

The valence molecular orbitals of nickel carbonyl accessible with 21.2175 eV radiation are shown schematically in fig. 1.

3.1. $9T_2$ and 2E states ("d" bands)

The $9t_2$ and 2e molecular orbitals originate from a splitting of the five degenerate d orbitals under the tetrahedral field. Evidence for π backbonding through the transition metal d orbitals, therefore, should be sought in the $9T_2$ and 2E photoelectron bands, which are presented in fig. 2. A reduction in the ν_2 (primarily Ni–C symmetric stretch) frequency from the 0.047

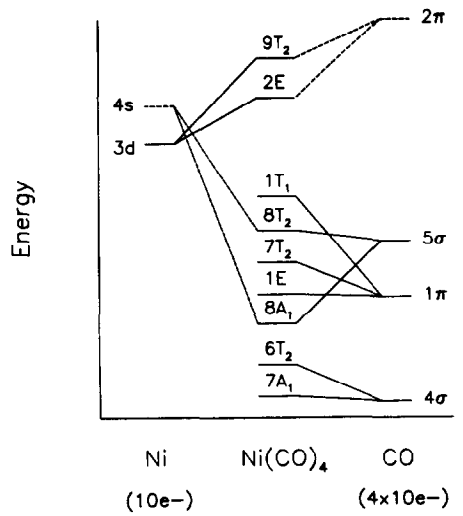

Fig. 1. The molecular orbitals of $Ni(CO)_4$ accessible with 21.2175 eV photons are represented schematically by the splitting of the atomic nickel and molecular CO levels within the T_d field.

eV value for the neutral molecule would be taken as clear evidence for the π-bonding character of these molecular orbitals. The photoelectron bands are very diffuse, however, and neither a second derivative analysis nor Fourier filtering of the photoelectron bands could elucidate vibrational fine structure above the

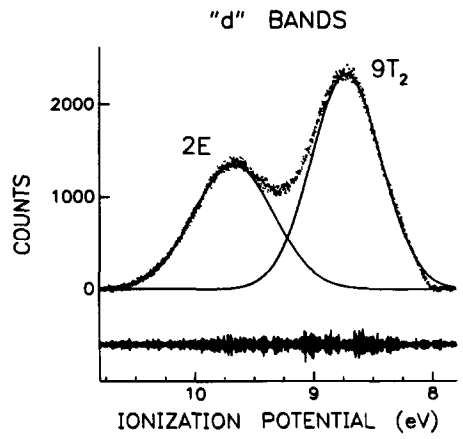

Fig. 2. The 21.2175 eV photoelectron spectrum of the $Ni(CO)_4$ "d" bands is plotted above with the results of a linear least-squares fit of the bands to two Gaussians. The second derivative of the Fourier-filtered spectrum is plotted below, revealing the absence of vibrationally resolved structure at this resolution (12 meV).

noise level. Three explanations are available for the absence of vibrational structure in the photoelectron bands of rotationally and vibrationally cold nickel carbonyl:

(i) Direct dissociation accompanies the loss of the photoelectron, resulting in featureless bands.

(ii) Ultra-fast relaxation processes broaden individual spectral features, resulting in a diffuse spectrum.

(iii) A dramatic change in the equilibrium geometry of the molecular ion from that of the neutral molecule results in a dense and unresolvable vibrational manifold.

The onset for the first dissociative ionization process:

$$Ni(CO)_4 + h\nu \rightarrow Ni(CO)_3^+ + CO + e^-$$

occurs at 8.77(2) eV [13], 0.75(3) eV above the $9T_2$ adiabatic ionization potential. Thus direct dissociation cannot explain the absence of vibrational structure. Since internally excited species are generally associated with ultra-fast relaxation processes, relaxation is an unlikely explanation for the diffuse threshold region. We turn, therefore, to the vibrational manifolds, as determined by the vibrational selection rules governing the photoionization process for the molecular geometries involved.

A normal-coordinate analysis of nickel carbonyl characterized the nine fundamental frequencies of the neutral molecule [14]. Vibrational selection rules and Franck–Condon factors limit the number of vibrational levels which will be observed in the photoelectron spectrum. If the resulting ion is of T_d symmetry, only the ν_1 (primarily the CO symmetric stretch) and ν_2 (primarily the M–C symmetric stretch) modes will be significantly excited in the photoionization of cold molecules. These vibrational modes have frequencies (ν_1 = 0.264 and ν_2 = 0.047 eV for the neutral [15]) that would be easily resolved by our photoelectron spectrometer. The additional complication of spin–orbit splitting of the d bands ($\lambda \approx 0.080$ eV [16]) will double these levels, but this alone will not prevent a vibrational analysis. The diffuse photoelectron bands indicate population of additional vibrational modes of the photoion, resulting from a strong distortion from a tetrahedral geometry. Both the $9T_2$ and 2E electronic states of $Ni(CO)_4^+$ are degenerate and unstable in a T_d configuration with respect to vibrations of species e [17].

A lowering of T_d symmetry to a D_{2d} symmetry for the molecular ion would be accompanied by strong excitations of the ν_4 mode (e symmetry), which is a C–Ni–C bending motion. This frequency is only 79 cm^{-1} (0.0098 eV) [15] for the neutral molecule, less than the instrumental resolution for this experiment. Significant excitation of the ν_4 mode, effected by a $D_{2d} \leftarrow T_d$ change in equilibrium geometry upon photoionization, is needed to explain the diffuse $9T_2$ and 2E photoelectron bands.

Minimum-internal-energy geometries for an $M(CO)_4$ species with d^9 and d^{10} electron configurations have been determined by EHMO [18,19] and LCAO MO [20] calculations. The calculations agree on a T_d geometry for a d^{10} species, as in the case of $Ni(CO)_4$. For a d^9 system, as in the case of the $9T_2$ state of $Ni(CO)_4^+$, refs. [18,20] agree on a D_{2d} equilibrium structure, while ref. [19] finds D_{2d} and C_{3v} structures to be minimum and energetically equivalent. The change in energy of the predominantly metal d orbitals with respect to geometry (Walsh diagrams) indicates that a distortion from T_d symmetry will also occur for the 2E state of $Ni(CO)_4^+$. Detailed minimum internal energy calculations have not been reported for the 2E state, however.

The diffuse $9T_2$ and 2E photoelectron bands are interpreted as manifestations of a strong distortion from T_d symmetry. The experimental and theoretical evidence support a D_{2d} structure for these states. A least-squares fit of the bands to two Gaussians, representing the two electronic states, was performed to determine the distribution of internal energies of the photoions. The near 3:2 intensity ratio for the two photoelectron bands (we measure 3:2.04) closely matches the degeneracy ratio, and this had assisted in the original assignment of the photoelectron bands [21]. The similar band shapes for the two electronic states, $9T_2$ (fwhm = 0.692 eV) and 2E (fwhm = 0.794 eV), indicate similar bonding strengths for the molecular orbitals. The band widths denote population of higher frequency vibrations, in addition to the ν_4 levels, and support the π-backbonding character of these molecular orbitals.

3.2. $1T_1$, T_2, $7T_2$, $1E$, $8A_1$, $6T_2$, $7A_1$ states ("CO" bands)

The seven electronic states derived from emission

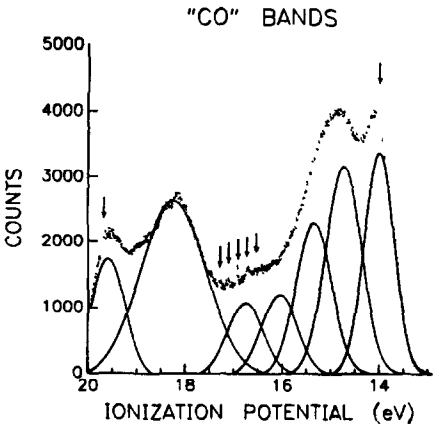

Fig. 3. The 21.2175 eV photoelectron spectrum of the "CO" bands is plotted together with the results of the linear least-squares fit to seven Gaussians. All fitting parameters are given in table 1. The arrows denote peaks resulting from the CO impurity in the beam.

from orbitals of predominantly CO character comprise the photoelectron spectrum in the 13–20 eV region. This complex spectral region is presented in fig. 3. In the earlier photoelectron spectroscopy investigation by Hillier, Guest, Higginson and Lloyd a partial assignment of the photoelectron bands was made on the basis of ab initio SCF MO calculations [21]. The $8T_2$, $1T_1$, 1E, and $7T_2$ states were assigned to the 15.5 eV region and the 15.7 eV shoulder was identified as the $8A_1$ state. The higher ionization potential features in the 18–20 eV range were assigned to the $6T_2$ and $7A_1$ states. Electron correlation and orbital relaxation introduce substantial error into the calculations, however, preventing a detailed assignment of the photoelectron bands. More recent theoretical studies employing $X\alpha$ scattered wave discrete variational and SCF HFS calculations have failed to agree on the relative ordering of the $8t_2$, $1t_1$, 1e, $7t_2$, and $8a_1$ molecular orbitals [3].

In cases where the localization properties of molecular orbitals do not vary significantly, the orbital degeneracies may be related to the relative intensities of photoelectron bands and assist in spectral assignments [22]. Angular distribution effects may introduce an error of up to 25% in the relative intensity versus degeneracy relationship. A linear least-squares fit of the photoelectron spectrum in the 13–20 eV region was performed with seven Gaussian functions

Table 1
Experimental and calculated assignment of $Ni(CO)_4^+$ outer valence electronic states (eV)

Electronic state	Vertical IP (from Gaussian) mean)	Band fwhm	Relative intensity	% error intensity/ degeneracy	Former expt. a)	Calculation		
						SCFS b)	SCF DV Xα c)	HF d) (Koopmans')
$9T_2(3d)$	8.722(10)	0.692	0.25	2	8.9	11.7	9.3	10.8
2E(3d)	9.674(10)	0.794	0.17	2	9.8	13.0	10.3	7.0
$1T_1(1\pi)$	14.009(20)	0.718	0.57	15	14.1	16.7	14.1 ($8T_2$)	17.5 ($8T_2$)
$8T_2(5\sigma)$	14.740(20)	0.855	0.64	7	14.9	17.0	14.6 ($1T_1$)	17.8 ($1T_1$)
$7T_2(1\pi)$	15.351(20)	0.859	0.47	3		17.0 (1E)	15.0 ($8A_1$)	18.0 ($7T_2$)
$1E(1\pi)$	16.058(20)	0.869	0.25	22		17.0 ($7T_2$)	15.0 ($7T_2$)	18.1 (1E)
$8A_1(5\sigma)$	16.756(20)	0.880	0.23	7	15.7	17.6	15.1 (1E)	18.9
$6T_2(4\sigma)$	18.252(20)	1.580	1.00	7	18.2	19.3	16.5	21.6
$7A_1(4\sigma)$	19.599(20)	0.837	0.36	7	19.7	20.4	17.2	22.0

a) Ref. [21]. b) Ref. [3]. c) Ref. [2]. d) Ref. [4].

representing the seven electronic states. More accurate vertical ionization potentials have been obtained by this method and the relative intensities are most consistent with an electronic state ordering of $1T_1(1\pi)$, $8T_2(5\sigma)$, $7T_2(1\pi)$, $1E(1\pi)$, $8A_1(5\sigma)$, $6T_2(4\sigma)$, and $7A_1(4\sigma)$. These results are summarized in table 1 and compared with theoretical calculations. The electronic states produced by the emission of 1π-derived molecular orbitals are seen to overlap and alternate in energy with the electronic states of primarily 5σ origin. Although the SCF DV Xα calculations offer the best agreement with observed ionization potentials, the ordering of electronic states determined from the SCFS calculations is most consistent with the present assignment of electronic states. More accurate calculations including configuration interaction are necessary to account for the severe electron correlation and orbital relaxation effects and provide a reasonable theoretical comparison for the experimentally observed sequence.

Acknowledgement

This work was supported by the Director, Office of Energy Research, Office of Basic Energy Sciences, Chemical Sciences Division of the US Department of Energy under contract No. DE-AC03-76SF00098.

References

[1] M. Wrighton, Chem. Rev. 74 (1974) 401.
[2] E.J. Baerends and P. Ross, Mol. Phys. 30 (1975) 1735.
[3] B.-I. Kim, H. Adachi and S. Imoto, J. Electron Spectry. 11 (1977) 349.
[4] I.H. Hillier and V.R. Sanders, Mol. Phys. 22 (1971) 1025.
[5] K.H. Johnson and U. Wahlgren, Intern. J. Quantum Chem. 6 (1972) 243.
[6] L.H. Jones, R.S. McDowell and M. Goldblatt, J. Chem. Phys. 48 (1968) 2663; Inorg. Chem. 8 (1969) 2349.
[7] F.A. Cotton and R.M. Wing, Inorg. Chem. 4 (1965) 314.
[8] J.L. Hubbard and D.L. Lichtenberger, J. Am. Chem. Soc. 104 (1982) 2132.

[9] J.E. Pollard, D.J. Trevor, Y.T. Lee and D.A. Shirley, Rev. Sci. Instr. 52 (1981) 1837.
[10] A. Amirav, U. Even and J. Jortner, Chem. Phys. 51 (1980) 31.
[11] G. Luijks, S. Stolte and J. Reuss, Chem. Phys. 62 (1981) 217.
[12] G. Luijks, S. Stolte and J. Reuss, Chem. Phys. Letters 94 (1983) 48.
[13] G. Distefano, J. Res. Natl. Bur. Std. 74A (1970) 233.
[14] H. Murata and K. Kawai, J. Chem. Phys. 26 (1957) 1355.
[15] L.H. Jones, J. Chem. Phys. 28 (1958) 1215.
[16] J.S. Griffith, The theory of transition metal ions (Cambridge Univ. Press, Cambridge, 1971).
[17] G. Herzberg, Molecular spectra and molecular structure, Vol. 3 (Van Nostrand Reinhold, New York, 1966).
[18] M. Elian and R. Hoffman, Inorg. Chem. 14 (1975) 1058.
[19] D.A. Pensak and R.J. McKinney, Inorg. Chem. 18 (1979) 3407.
[20] J.K. Burdett, J. Chem. Soc. Faraday Trans. II 70 (1974) 1599.
[21] I.H. Hillier, M.F. Guest, B.R. Higginson and D.R. Lloyd, Mol. Phys. 27 (1974) 215.
[22] A.H. Cowley, Progr. Inorg. Chem. 26 (1979) 46.